



Keywords:

Stokes drift, surface gravity waves, Lagrangian dynamics, wave groups

Author for correspondence:

T.S. van den Bremer
ton.vandenbremer@ed.ac.uk

Lagrangian transport for two-dimensional deep-water surface gravity wave groups

T.S. van den Bremer^{1,2} and P.H. Taylor²

1. School of Engineering, University of Edinburgh, Robert Stevenson Road, Edinburgh, EH9 3FB (UK)
2. Department of Engineering Science, University of Oxford, Parks Road, Oxford, OX1 3PJ (UK)

The Lagrangian trajectories of neutrally buoyant particles underneath surface gravity wave groups are dictated by two physical phenomena: the Stokes drift results in a net displacement of particles in the direction of propagation of the group, whereas the Eulerian return flow, as described by the multi-chromatic wave theory of Longuet-Higgins & Stewart (1962), transports such particles in the opposite direction. By pursuing a separation of scales expansion, we develop simple closed-form expressions for the net Lagrangian displacement of particles. By comparing the results from the separation of scales expansion at different orders in bandwidth, we study the effect of frequency dispersion on the local Lagrangian transport, which we show can be ignored for realistic sea states.

1. Introduction

The net horizontal movement that a fluid particle undergoes in a water wave, named Stokes drift after Sir George Gabriel Stokes who first derived a theoretical description for this drift in 1847, has been studied extensively. Taking a Lagrangian approach, [Stokes \(1847\)](#) found the following expression for the horizontal drift velocity for regular waves in deep water and to second order of approximation:

$$u_{SD}(z_0) = \frac{1}{T} \int_t^{t+T} u(x(t), z(t), t) dt = c(ka)^2 e^{2kz_0}, \quad (1.1)$$

where $c = \sqrt{g/k}$ is the wave celerity, g is the gravitational constant, $k = 2\pi/\lambda$ is the wave number of the regular wave, a its amplitude, T its period and z_0 the initial vertical position of the particle with $z_0 = 0$ corresponding to the still water level. Stokes drift is thus a non-linear phenomenon (cf. $(ka)^2$) that can be derived entirely from linear theory. [Stokes \(1847\)](#) considered both the effect of horizontal displacement $x(t) = x_0 + \Delta x(t)$ and the vertical displacement $z(t) = z_0 + \Delta z(t)$ on the drift velocity u_{SD} , equal to the net displacement per wave period T , and found that half of the drift arose from each. The resulting close to circular particle orbits with orbits near the surface not quite closing are illustrated by Wallet & Ruellan's (1950) image reproduced in [van Dyke's \(1982\)](#) Album of Fluid Motion. In an Eulerian framework ([Starr, 1947](#)), a net mass flux is identified by integrating the (linear) horizontal velocity from the bottom $z \rightarrow -\infty$ up to the (linear) free surface $z = \eta(x, t)$. Because the horizontal velocity is higher at a crest than at a trough, the result gives a mean depth-integrated horizontal flux consistent with the flux obtained by depth integration of (1.1):

$$Q_{ST} = \frac{1}{T} \int_t^{t+T} \int_{-\infty}^{\eta(x,t)} u(x(t), z(t), t) dz dt = \frac{1}{2} \sqrt{\frac{g}{k^3}} (ka)^2, \quad (1.2)$$

a volume flux that is sometimes referred to as the ‘‘Stokes transport’’ and is therefore abbreviated by the subscript ST.

Stokes drift is thought to play an important role in the physics of ocean surfaces and hence constitutes an important component of oceanic general circulation models (OGCMs) ([Belcher *et al.*, 2012](#); [McWilliams & Restrepo, 1999](#)). In particular, it is now widely accepted that the interaction between Stokes drift induced by surface waves and vertical shear in turbulent fluid is responsible for Langmuir circulation ([Craig & Leibovich, 1976](#)). In turn, Langmuir circulation is a large contributor of turbulent kinetic energy to the upper mixed layer of the ocean surface, much larger than for example wave breaking ([Kantha & Clayson, 2004](#)). Many authors have estimated Stokes drift and its geographical spatial distribution across the world's seas and oceans from oceanographic datasets (e.g. [Smith \(2006\)](#), [Ardhuin *et al.* \(2009\)](#) and [Tamura *et al.* \(2012\)](#)). Typically, such studies are concerned with the dynamics at the surface only and are based on linear wave theory. In oceanic general circulation models, in which the shear of the Stokes drift velocity needs to be included to model Langmuir turbulence, it is customary to replace the full Stokes drift velocity profile by a monochromatic profile matched to the transport and the surface Stokes velocity to avoid expensive computations. [Breivik *et al.* \(2014\)](#) have recently proposed alternative simple approximations based on the deep-water assumption that take into account the group structure of real seas.

Other authors have considered Stokes drift for periodic waves in experimental wave flumes (e.g. [Swan \(1990\)](#), [Hudspeth & Sulisz \(1991\)](#), [Monismith *et al.* \(2007\)](#)) and have found that in such closed domains in which the zero net mass flux constraint is automatically satisfied, Stokes drift has to be accompanied, at least in the depth-integrated sense, by an Eulerian return current typically driven by a setup in the direction downstream of wave propagation. Surprisingly, [Monismith *et al.* \(2007\)](#), who study periodic waves in a closed tank, observe that the Stokes drift is not only cancelled by an Eulerian current in the depth-integrated sense, but that a cancellation takes place at all levels. Based on these observations [Monismith *et al.* \(2007\)](#) hypothesize the existence of (rotational) Gerstner waves in wave tank experiments, an hypothesis further discussed in [Weber \(2011\)](#), but not explored herein. The difference between laboratory measurements and the predictions of the mass-transport velocity predicted by [Stokes \(1847\)](#) based on irrotational flow was

already noted by Longuet-Higgins (1953). Vorticity is advected or diffused from the boundary layers at the bottom, sides or ends of the flume into the interior of the fluid invalidating the assumption of irrotational flow. When regular waves are first generated in a laboratory flume, the interior of the fluid will be first irrotational until vorticity is transported and a different solution is established (see Groeneweg & Klopman (1998) for a comparison of the solutions of Longuet-Higgins (1953) with experimental results).

In practice, the wave field on the open sea often has a group-like structure. The structure of the wave-induced mean flow is fundamentally different for wave groups compared to regular waves. As the group travels on a faster time scale than the time scale on which vorticity can be diffused from the bottom boundary layer (Longuet-Higgins's (1953) "conduction" solution) or advected by the mean flow (Longuet-Higgins's (1953) "convection" solution), the interior of the flow underneath the wave group remains irrotational. In physical terms, the Stokes transport flux (1.2) is divergent on the scale of the group and must induce another flow at second order: the return flow. In mathematical terms, the different wave number components, which make up the linear multi-chromatic wave group, interact to produce frequency-sum and frequency-difference components at second order in amplitude. The frequency-difference components, in turn, are responsible for the return flow, as first described by Longuet-Higgins & Stewart (1962). For deep water, a spatial separation of the two effects takes place: the Stokes transport dominates at the free surface over the e-folding depth $(2k_0)^{-1}$ with k_0 now denoting the peak of the wave number spectrum; the magnitude of the return flow decreases much more slowly with depth and consequently dominates far below the free surface. Combining the (local) Stokes transport and the (non-local) return flow leads to zero vertically-integrated mass transport at the centre of the group and hence there is zero vertically-integrated momentum associated with the centre of a surface gravity wave group, as emphasized by McIntyre (1981).

As time-integration of the double-Fourier solutions for the return flow, as documented in Longuet-Higgins & Stewart (1962), Sharma & Dean (1981) or Dalzell (1999), with their slowly decaying tails is numerically non-trivial, we instead pursue a separation of scales expansion between the slow or long scales of the group and the fast or short scales of the individual waves. We develop simple expressions for the net Lagrangian displacement of particles as a function of steepness and bandwidth and study its variation with depth. By considering subsequent orders in the expansion, we study the effects of frequency dispersion and compare to the solutions of Longuet-Higgins & Stewart (1962). In doing so, we justify the ad-hoc assumption made in van den Bremer & Taylor (2015) to only consider the leading-order term in the separation of scales expansion that was shown to give simple results for finite depth and directional spreading. Finally, we examine the Lagrangian trajectories of neutrally buoyant particles underneath focussed surface gravity wave groups in two-dimensionally infinitely deep seas.

This paper is laid out as follows. The governing equations and notation are introduced in §2 followed by the introduction of the perturbation expansion framework in §3. The equations describing the Stokes drift and the return flow are solved and discussed in §4. Lagrangian particle trajectories are then examined in §5 followed by conclusions in §6.

2. Governing equations

A two-dimensional body of water of infinite depth and indefinite lateral extent is assumed with a coordinate system (x, z) , where x denotes the horizontal coordinate and z the vertical coordinate measured from the undisturbed water level upwards. Inviscid, incompressible and irrotational flow is assumed and, as a result, the velocity vector can be defined as the gradient of the velocity potential $\mathbf{u} = \nabla\phi$. The governing equation within the domain of the fluid is then Laplace:

$$\nabla^2\phi = 0 \quad \text{for } z \leq \eta(x, t), \quad (2.1)$$

where $\eta(x, t)$ denotes the free surface. The kinematic and dynamic free surface boundary conditions are, respectively:

$$w - \frac{\partial\eta}{\partial t} - u\frac{\partial\eta}{\partial x} = 0, \quad g\eta + \frac{\partial\phi}{\partial t} + \frac{1}{2}(u^2 + w^2) = 0 \quad \text{at } z = \eta(x, t), \quad (2.2a, b)$$

where gravity g acts in the negative z direction. Finally, there is a no-flow bottom boundary condition requiring that $\partial\phi/\partial z = 0$ as $z \rightarrow -\infty$. We combine the two free surface boundary conditions (2.2a,b) into one equation in terms of ϕ :

$$\frac{\partial^2 \phi}{\partial t^2} + g \frac{\partial \phi}{\partial z} + \frac{\partial}{\partial t} \left(\left(\frac{\partial \phi}{\partial x} \right)^2 + \frac{1}{2} \left(\frac{\partial \phi}{\partial z} \right)^2 \right) + \frac{1}{2} \frac{\partial \phi}{\partial x} \frac{\partial}{\partial x} (\nabla \phi)^2 = 0 \quad \text{at } z = \eta(x, t), \quad (2.3)$$

3. Perturbation expansion for wave groups

In this section we will derive a forcing equation for the return flow at second order in steepness. Whereas one small parameter (the wave steepness α) is sufficient to examine periodic waves, two small parameters are required for the study of wave groups by means of a perturbation expansion: a steepness parameter α and a bandwidth parameter ϵ separating slow and fast scales. We define $\alpha \equiv k_0 |A_0|$, where $|A_0|$ is the magnitude (of the leading-order component in bandwidth, see §3(a)) of the complex envelope of the surface elevation η and k_0 is the wave number of the (fast) carrier wave. The fast spatial and temporal scales are denoted by x , z and t and the slow scales by:

$$X = \epsilon(x - c_g t), \quad Z = \epsilon z, \quad T = \epsilon^2 t, \quad (3.1a,b,c)$$

where the slow scale X translates with the group velocity. We also require the slow vertical scale Z to ensure our solution satisfies its governing equation (Laplace) at all orders in (see §3(a)) and the higher-order time scale T to capture the effects of frequency dispersion causing the group to be no longer steady in its own reference frame, but widen. The bandwidth parameter ϵ is defined as proportional to the ratio of the wave length of the carrier wave λ_0 and the characteristic length of the group σ , namely $\epsilon \equiv 1/(k_0 \sigma)$. We keep track of both the order in the bandwidth parameter ϵ , which we denote by a subscript, and the order in the steepness of the signal, which we denote by a superscript. For example, $\eta_{(1)}^{(2)}$ denotes the component of the surface elevation that is first order in bandwidth ϵ and second order in steepness α . Although it is formally necessary to define a relationship between the small parameters in a relationship so that the terms can be ranked, we do not make the assumption that $\epsilon = \alpha$, an assumption that is commonly made to derive equations of the non-linear Schrödinger type (e.g. Dysthe (1979)). This allows us to give a physical interpretation to the different terms.

We note different authors have adopted different symbols and conventions to denote the group. For example, in Yuen & Lake (1975), a denotes the magnitude of the complex amplitude of the surface elevation A so that $A = a \exp(i\tilde{\theta})$, whereas in Dysthe (1979) A denotes the complex amplitude of the velocity potential and B denotes the complex amplitude of the surface elevation. Yuen & Lake (1975) then continue to express their equations in terms of the (complex) amplitude of the surface elevation, whereas Dysthe (1979) has his in terms of the (complex) amplitude of the velocity potential. Herein, we adopt the following inelegant but consistent notation. We let B denote the complex amplitude envelope of the velocity potential ϕ (with dimensions $L^2 T^{-1}$). Similarly, A_n denotes the complex amplitude of the surface elevation (with dimensions L) at n th order in bandwidth ϵ . We then use $\partial/\partial x$ to denote the combined effect of slow and fast derivatives, but let the subscripts in ∂_x and ∂_X denote only fast or slow derivatives, respectively. We restrict our attention to first and second order in steepness α , which we consider in turn.

(a) Linear in steepness $O(\alpha)$

We consider the following linear (in steepness) velocity potential:

$$\phi^{(1)}(x, z, t) \equiv \phi_{(0)}^{(1)}(x, z, t) \equiv \text{Re} [B(X, Z, T) e^{k_0 z} e^{i(k_0 x - \omega_0 t)}], \quad (3.2)$$

with $\phi_{(n)}^{(1)} \equiv 0$ for $n \geq 1$. Equation (3.2) automatically satisfies Laplace (2.1) at $O(\alpha^1 \epsilon^0)$ and for subsequent orders in ϵ we obtain: $\partial_Z B = -i \partial_X B$ and $\partial_{ZZ} B = -\partial_{XX} B$ for $z \leq 0$. From the combined free surface boundary condition (2.3) we obtain, at subsequent orders in ϵ , the linear dispersion relationship ($\alpha^1 \epsilon^0$), the group velocity at which the envelope travels without changing shape ($\alpha^1 \epsilon^1$) and the modification to this shape due

to leading-order dispersion ($\alpha^1 \varepsilon^2$):

$$\underbrace{(gk_0 - \omega_0^2)}_{=0} B + 2i\varepsilon\omega_0 \underbrace{\left(c_{g,0} - \frac{g}{2\omega_0}\right)}_{=0} \partial_X B + \varepsilon^2 \underbrace{(c_{g,0}^2 \partial_{XX} - 2i\omega_0 \partial_T)}_{=0} B = 0 \quad \text{at } z = 0, \quad (3.3)$$

where we have used $\partial_Z B|_{z=0} = -i\partial_X B|_{z=0}$ from Laplace at $O(\alpha^1 \varepsilon^1)$. The linearized (in α) version of (2.2a), $\partial\eta/\partial t = \partial\phi/\partial z|_{z=0}$, provides a relationship between $\phi^{(1)}$ in (3.2) and $\eta^{(1)}$. The latter is defined as:

$$\eta^{(1)} \equiv \sum_{n=0}^{\infty} \eta_{(n)}^{(1)} \equiv \sum_{n=0}^{\infty} A_n \varepsilon^n e^{i(k_0 x - \omega_0 t)}, \quad (3.4)$$

where A_n (with units L) denotes the envelope of the $O(\alpha \varepsilon^n)$ component of the surface elevation $\eta_{(n)}^{(1)}$. From (2.2a) we then have:

$$\left(\partial_t - \varepsilon c_{g,0} \partial_X + \varepsilon^2 \partial_T\right) \sum_{n=0}^{\infty} \eta_{(n)}^{(1)} = \left(k_0 - i\varepsilon \partial_X\right) B|_{z=0} e^{i(k_0 x - \omega_0 t)}, \quad (3.5)$$

where we have used $\partial_Z B|_{z=0} = -i\partial_X B|_{z=0}$ from Laplace at $O(\alpha^1 \varepsilon^1)$. In order to satisfy (2.2a) at first order in α and all orders in ε , it can be shown that we need an infinite number of terms in (3.4). The first three terms are:

$$A_0 = i \frac{k_0}{\omega_0} B|_{z=0}, \quad A_1 = \frac{1}{2} \frac{1}{\omega_0} \partial_X B|_{z=0}, \quad A_2 = \frac{1}{\omega_0^2} \left(\frac{i}{2} c_{g,0} \partial_{XX} + k_0 \partial_T \right) B|_{z=0}. \quad (3.6a,b,c)$$

(b) Second-order in steepness $O(\alpha^2)$

At $O(\alpha^2)$ we have from (2.2):

$$\begin{aligned} \frac{\partial\phi^{(2)}}{\partial z} + \frac{\partial^2\phi^{(1)}}{\partial x^2} \eta^{(1)} - \frac{\partial\eta^{(2)}}{\partial t} - \frac{\partial\phi^{(1)}}{\partial x} \frac{\partial\eta^{(1)}}{\partial x} &= 0 \quad \text{at } z = 0, \\ g\eta^{(2)} + \frac{\partial\phi^{(2)}}{\partial t} + \frac{\partial^2\phi^{(1)}}{\partial t \partial z} \eta^{(1)} + \frac{1}{2} \left(\left(\frac{\partial\phi^{(1)}}{\partial x} \right)^2 + \left(\frac{\partial\phi^{(1)}}{\partial z} \right)^2 \right) &= 0 \quad \text{at } z = 0. \end{aligned} \quad (3.7a,b)$$

We have from combination of (3.7a) (3.7b) and at $O(\alpha^2)$:

$$\left(\frac{\partial}{\partial z} + \frac{1}{g} \frac{\partial^2}{\partial t^2} \right) \phi^{(2)} = \frac{\partial}{\partial x} \left(\eta^{(1)} \frac{\partial\phi^{(1)}}{\partial x} \right) - \frac{1}{g} \frac{\partial}{\partial t} \left(\frac{\partial^2\phi^{(1)}}{\partial z \partial t} \eta^{(1)} + \frac{1}{2} \left(\left(\frac{\partial\phi^{(1)}}{\partial x} \right)^2 + \left(\frac{\partial\phi^{(1)}}{\partial z} \right)^2 \right) \right) \quad \text{at } z = 0, \quad (3.8)$$

where we have used $\partial^2\phi^{(1)}/\partial z^2 = -\partial^2\phi^{(1)}/\partial x^2$ from Laplace. Equation (3.8) can be understood as the “forcing equation” of the return flow with its right-hand side terms representing a “forcing” by the products of first-order (in steepness) wave terms that gives rise to a mean flow on the left hand side. In fact, it can be shown by substituting the $O(\alpha)$ solutions at the various orders in ε into the right hand side that the “forcing” only gives rise to mean flow terms and that there are no higher harmonics for the potential (at least up to $O(\alpha^2 \varepsilon^3)$). Equation (3.8) becomes:

$$\left(\varepsilon \partial_Z + \frac{1}{g} \varepsilon^2 c_{g,0}^2 \partial_{XX} \right) \phi_{\text{RF}}^{(2)}(X, Z, T) = \frac{\varepsilon k_0^2}{2\omega_0} \partial_X |B|^2 + O(\alpha^2 \varepsilon^3) \quad \text{at } z = 0, \quad (3.9)$$

where we note that the forcing term at $O(\alpha^2 \varepsilon^2)$, the order of leading-order dispersion in (3.3), is equal to zero. The return flow can thus be found by solving its governing equation $(\partial_{XX} + \partial_{ZZ})\phi_{\text{RF}}^{(2)} = 0$ subject to (3.9) and the bottom boundary condition. We note that our (3.9) up to $O(\varepsilon^2)$ is equivalent to (2.20-2.21) of Dysthe (1979), who sets $\alpha = \varepsilon$ and only considers terms up to 4th order in the combined small parameter.

4. Stokes drift, transport and the return flow for wave groups

Having derived a forcing equation for the return flow (3.9) in the previous section, this section evaluates the explicit solutions for the Stokes drift and transport and the return flow at the different orders in ε . It first ignores the effects of dispersion (§4(a)), then includes leading-order dispersion (§4(b)) and finally incorporates all linear (in steepness) dispersion to reproduce the Fourier-space solutions of Longuet-Higgins

& Stewart (1962) (§4(c)). To assess the effect of frequency dispersion comparisons are made between the three solutions for a Gaussian spectrum that is reasonably broad-banded ($\epsilon = 0.16$). The value $\epsilon = 0.16$ is representative of a severe sea state and is obtained by fitting a Gaussian distribution to the peak of a JONSWAP spectrum obtained from measurements of real seas (Hasselmann *et al.*, 1980) with a peak enhancement factor $\gamma = 3.3$ (Gibbs & Taylor, 2005).

(a) Wave groups without dispersion $O(\alpha^2\epsilon^1)$

(i) Stokes drift and transport for groups without dispersion $O(\alpha^2\epsilon^0)$

By substituting the leading-order ($\alpha^1\epsilon^0$) solutions for the horizontal and vertical velocity u and w into the differential equation for the Lagrangian particle position, a leading-order ($\alpha^2\epsilon^0$) expression for the Stokes drift and transport can be derived. The horizontal Stokes drift velocity and the Stokes transport become:

$$u_{SD}(x, z, t) \equiv \overline{\frac{\partial u^{(1)}}{\partial x} \Delta x^{(1)} + \frac{\partial u^{(1)}}{\partial z} \Delta z^{(1)}} = \omega_0 k_0 e^{2k_0 z} |A_0(X)|^2, \quad Q_{ST}(x, t) \equiv \overline{u^{(1)} \eta^{(1)}} = \frac{1}{2} \omega_0 |A_0(X)|^2, \quad (4.1a, b)$$

where $\Delta x^{(1)}$ and $\Delta z^{(1)}$ are the linear displacement fields and the overlines denote averaging over the fast scales. Comparison with (1.1) and (1.2) for periodic waves immediately reveals, not surprisingly, that (4.1a) and (4.1b) are direct extensions of the periodic case with the amplitude envelope A_0 , which varies on the slow scales, replacing the constant amplitude $H/2$. The Stokes transport Q_{ST} now increases (with increasing x) at the trailing edge of the group and decreases at the leading edge. It does so at the slow length scale X associated with the group and in doing so, it effectively “absorbs” fluid at the trailing edge, transports it through the centre of the group and deposits it at the leading edge of the group. In other words, the Stokes transport is not divergence-free. The local “excess” quantity of fluid thus generated near the free surface is given by $-\partial Q_{ST}/\partial x$. In physical terms, this excess (or deficit) necessitates a return flow. In the classical interpretation, the return flow is driven by a gradient in the radiation stresses (Longuet-Higgins & Stewart, 1964; McIntyre, 1981).

(ii) Return flow for groups without dispersion $O(\alpha^2\epsilon^1)$

At leading order in ϵ , the return flow can be found by solving for the potential flow field in the infinite half-space subject to the boundary conditions $w_{RF} \rightarrow 0$ as $z \rightarrow -\infty$ and from (3.9):

$$w_{RF}(X, Z=0) = \frac{1}{2} \omega_0 \epsilon \frac{\partial |A_0(X)|^2}{\partial X} = \epsilon \frac{\partial Q_{ST}(X)}{\partial X}, \quad (4.2)$$

where the second equality follows from (4.1b). It is evident then that the Stokes transport acts as a sink (and the return flow as a source) with fluid flowing upwards ($w_{RF}(X, Z=0) > 0$) when the volume flux transported by Stokes transport along the free surface increases along the trailing edge of the group ($\partial_X Q_{ST} > 0$ for $X < 0$). Conversely, the Stokes transport acts as a source (and the return flow as a sink) with excess fluid flowing downwards ($w_{RF}(X, Z=0) < 0$ for $X > 0$) when the volume flux transported by the Stokes transport along the free surface decreases along the leading edge of the group ($\partial_X Q_{ST} < 0$ for $X > 0$).

Using separation of variables and a Fourier sine transform for a Gaussian wave group $A_0(x, t) = a_0 \exp(-(x - c_{g,0}t)^2/2\sigma^2)$ to solve the boundary value problem $(\partial_{XX} + \partial_{ZZ})\phi_{RF}^{(2)} = 0$ subject to (4.2) and the bottom boundary condition, we obtain for the potential of the return flow:

$$\phi_{RF}(x, z, t) = -\frac{1}{2\sqrt{\pi}} |a_0|^2 \omega_0 \sigma \int_0^\infty e^{-\frac{1}{4}(k\sigma)^2 + kz} \sin(k(x - c_{g,0}t)) dk. \quad (4.3)$$

Alternatively, the return flow can be described by a summation of sinks and sources placed at the still water level $z = 0$ with the strength of the source given by $M = -\epsilon \partial_X Q_{ST}$:

$$u_{RF}(x, z, t) = \int_0^\infty \frac{M(l)}{\pi} \left[\frac{x - l - c_{g,0}t}{(x - l - c_{g,0}t)^2 + z^2} - \frac{x + l - c_{g,0}t}{(x + l - c_{g,0}t)^2 + z^2} \right] dl, \quad (4.4)$$

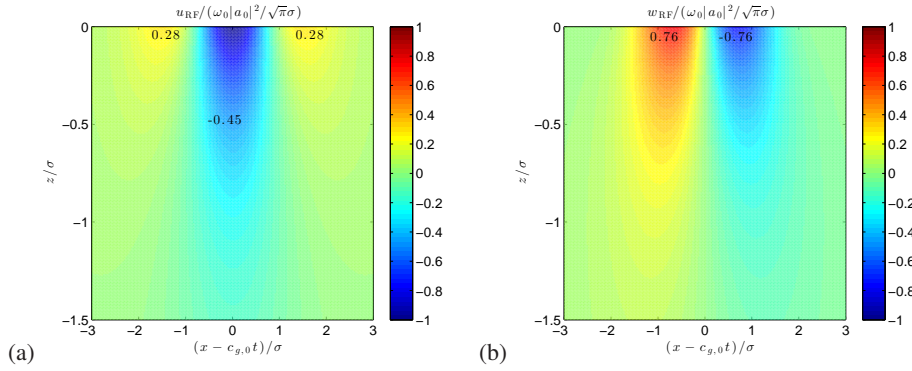


Figure 1. Return flow velocity field for wave groups without dispersion showing (a) the horizontal velocity and (b) the vertical velocity for $\varepsilon = 0.16$. It is evident from panel a that the “return” flow not only consists of negative horizontal velocities.

where the strength is given by $M(l) = (\omega_0 |a_0|^2 / \sigma) (l / \sigma) \exp(-l / \sigma)^2$, as evaluated from (4.1b) for a Gaussian group. We note that the expression for u_{RF} in (4.4) (evaluated at $z = 0$) can also directly be obtained by taking the Hilbert transform of in (4.2) (evaluated at $z = 0$) (Janssen, 1983). Although perhaps more physically intuitive, the resulting return flow is entirely equivalent to (4.3). Although the Stokes transport is distributed with depth, we note that for the purposes of forcing the return flow the sources and sinks can be located at the still water level (to the order of approximation considered here).

Figure 1 illustrates the spatial distribution of the horizontal and the vertical component of the return flow field, which at leading order are steady in the frame of reference of the group. It is evident from figure 1b that the return flow consist of downward and upward flowing bodies of fluid on, respectively, the leading and trailing edge of the group, consistent with the idea of a “return” flow. From figure 1a it is evident that the return flow not only consists of a large backward flow underneath the centre of the group $|x - c_{g,0}t| \lesssim 0.5\sigma$, but also sizeable forwards flow centered around $x - c_{g,0}t = \sqrt{2}\sigma$ at the leading edge and $x - c_{g,0}t = -\sqrt{2}\sigma$ at the trailing edge.

To examine the variation of the return flow with depth, consider the horizontal component of the return flow u_{RF} at the centre of the group $x = c_{g,0}t$, where $w_{\text{RF}} = 0$. From either (4.3) or (4.4) we have at this location, the only location at which a non-trivial closed-form solution is available (see appendix A):

$$u_{\text{RF}}(x = c_{g,0}t, z) = -\frac{\omega_0 |a_0|^2}{\sqrt{\pi}\sigma} \left(1 + \sqrt{\pi} \frac{z}{\sigma} \left(1 + \operatorname{erf}\left(\frac{z}{\sigma}\right) \right) e^{\frac{z^2}{\sigma^2}} \right), \quad (4.5)$$

which has the near-surface limit $|z| \ll \sigma$ and the deep-down limit $|z| \gg \sigma$:

$$u_{\text{RF}}(x = c_{g,0}t, z) = \begin{cases} -\frac{\omega_0 |a_0|^2}{\sqrt{\pi}\sigma} & \text{for } |z| \ll \sigma, \\ -\frac{\omega_0 |a_0|^2}{\sqrt{\pi}\sigma} \frac{1}{2} \left(\frac{z}{\sigma} \right)^{-2} & \text{for } |z| \gg \sigma. \end{cases} \quad (4.6)$$

More generally, we can derive the following limiting behaviour of the horizontal component of the return flow in the far-field of large $|x - c_{g,0}t|$ or large $|z|$ (see appendices B-C):

$$u_{\text{RF}}(x, z, t) = \frac{|a_0|^2 \sigma \omega_0}{2\sqrt{\pi}} \frac{(x - c_{g,0}t)^2 - z^2}{((x - c_{g,0}t)^2 + z^2)^2}, \quad (4.7)$$

from which we can obtain the two far-field limits: $u_{\text{RF}} \sim -z^{-2}$ for $|z| \gg |x - c_{g,0}t|$ and $u_{\text{RF}} \sim (x - c_{g,0}t)^{-2}$ for $|x - c_{g,0}t| \gg |z|$, where we emphasize the difference in sign. In the first limit, namely deep down in the fluid below the group, the horizontal flow velocity is negative, whereas near the surface, either far in

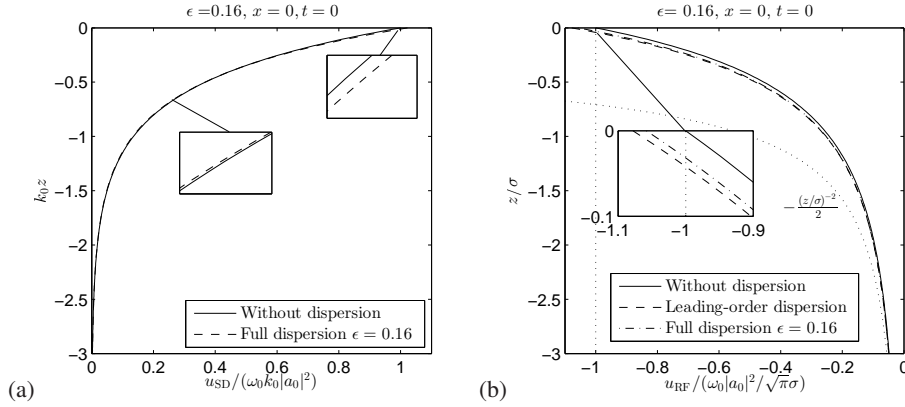


Figure 2. Stokes drift (a) and return flow (b) velocities for wave groups as a function of depth at the centre of the group $x = 0$ at $t = 0$, the time of focus, comparing the solutions for groups without dispersion, with leading-order dispersion and with full dispersion. Note the different scales on the axes: $z/\sigma = \epsilon(k_0 z)$ with $\epsilon = 0.16$ here. The dotted line in panel b corresponds to the asymptotic limits (4.6).

front or far behind the group, the horizontal flow velocity is positive. The horizontal flow is zero in the far field along 45° lines drawn from the centre of the group (4.7). It is also instructive here to note the difference in depth decay between the Stokes drift and the return flow: the Stokes drift (4.1) decays very rapidly (exponentially) with depth on the scale of the wave length of the individual waves λ_0 (cf. $\exp(2k_0 z)$) as opposed to the return flow which asymptotically decays much more slowly with depth (cf. $(z/\sigma)^{-2}$) on the scale of the width of the group σ . Figure 2 compares the depth decay of the Stokes drift and the return flow at the centre of the group. The horizontal velocity of the return flow (4.4) can be integrated with depth to obtain the total volume flux by the return flow:

$$Q_{\text{RF}} = \int_{-\infty}^0 u_{\text{RF}} dz = -\frac{1}{2} |a_0|^2 \omega_0 e^{\frac{(x-c_{g,0}t)^2}{\sigma^2}}, \quad (4.8)$$

thereby confirming the result, emphasized by McIntyre (1981), that $Q_{\text{RF}}(x, t) + Q_{\text{ST}}(x, t) = 0$, a (non-dispersive) surface gravity wave group is associated with zero depth-integrated momentum.

(b) Wave groups with leading-order dispersion $O(\alpha^2 \epsilon^2)$

From inspection of (3.9) it is clear that at the next order in bandwidth ($\alpha^2 \epsilon^2$), the order at which the leading-order effects of dispersion cause the group to change shape as it translates, the “forcing term” of the return flow is zero. It can indeed be confirmed from integrating the differential equation for particle position $d\mathbf{x}/dt = \mathbf{u}(\mathbf{x}, t)$ over the fast time scale but allowing for leading-order slow variation in Δx and Δz that no additional Stokes drift arises at order $\alpha^2 \epsilon$. Leading-order dispersion, however, causes the group to evolve differently in space and time. As time progresses the group becomes wider due to dispersion and the third term in (2.2) must now also be satisfied to reflect this. At this order we have for a Gaussian group (Kinsman, 1984):

$$B(x, z, t)|_{z=0} = -i \frac{\omega_0}{k_0} A_0(x, t) = b_0 \frac{1}{\sqrt{1 + \frac{i \gamma_0 t}{\sigma^2}}} e^{-\left(\frac{1}{1 + \gamma_0^2 t^2 / \sigma^4} \frac{(x - c_{g,0} t)^2}{2\sigma^2}\right)} e^{i \left(\frac{\gamma_0 t / \sigma^2}{1 + \gamma_0^2 t^2 / \sigma^4} \frac{(x - c_{g,0} t)^2}{2\sigma^2}\right)}, \quad (4.9)$$

with $\gamma_0 = d^2 \omega / dk^2|_{k=k_0} = -\sqrt{g/k_0^3}/4$ and $\omega(k)$ obtained from the linear dispersion relationship. More simply, we have for the magnitude of B :

$$|B(x, t)| = |\tilde{b}| e^{-\frac{(x - c_{g,0} t)^2}{2\sigma^2}}, \quad (4.10)$$

with $|\tilde{b}| = |b_0|/(1 + \gamma_0^2 t^2/\sigma^4)^{1/4}$ denoting the effective amplitude and $\tilde{\sigma} = \sigma\sqrt{1 + \gamma_0^2 t^2/\sigma^4}$ the effective Gaussian half-width of the group. As the group disperses with time, the group widens ($\partial\tilde{\sigma}/\partial t > 0$) and its effective amplitude decreases ($\partial|\tilde{b}|/\partial t < 0$). At any point in time, the forcing term on the right hand side of (3.9) can be modified to include the effects of leading-order dispersion by replacing σ by $\tilde{\sigma}$ and $|b|$ by $|\tilde{b}|$. We note in passing that (4.9) satisfies the linear part of the non-linear Schrödinger equation often used to model weakly non-linear, narrow-banded, deep-water wave groups. Furthermore, we note that although the small parameter ϵ , as defined here ($\epsilon \equiv 1/(k_0\sigma)$), stays constant as the group widens, the actual ratio of length scales $\tilde{\epsilon} \equiv 1/(k_0\tilde{\sigma})$ reduces. As a result, approximations based on the separation of scales approach become even more accurate at long times

Although the right hand side of (3.9) is not, the left hand side of (3.9) is affected by leading-order dispersion. Including the $O(\epsilon^2)$ term, we obtain without further approximation:

$$\phi_{\text{RF}}(x, z, t) = -\frac{1}{2\sqrt{\pi}}|\tilde{a}_0|^2\omega_0\tilde{\sigma}\int_0^\infty \frac{e^{-\frac{1}{4}(k\tilde{\sigma})^2+kz}\sin(k(x-c_{g,0}t))}{1-kc_{g,0}^2/g}dk, \quad (4.11)$$

where $|\tilde{a}_0| = |a_0|/(1 + \gamma_0^2 t^2/\sigma^4)^{1/4}$ is the effective amplitude. It is evident from figure 2b that leading-order dispersion slightly enhances the magnitude of the return flow. Comparison with the non-dispersive and the fully dispersive solution is made next.

(c) Fully dispersive wave groups $O(\alpha^2\epsilon^\infty)$

For completeness, we also follow the frequency domain approach of Longuet-Higgins & Stewart (1962) (see also Dalzell (1999); Sharma & Dean (1981)). In doing so, we not only capture the effect of leading-order frequency dispersion of the group (§4(b)), but effectively include all orders in ϵ . Instead of discretizing the spectrum (Longuet-Higgins & Stewart, 1962), we define the following linear (in steepness) velocity potential and surface elevation using a continuous spectrum:

$$\phi^{(1)}(x, z, t) = \int_{-\infty}^\infty \hat{b}(k)e^{k|z|}e^{i[kx-\omega(k)t]}dk, \quad \eta^{(1)}(x, t) = \int_{-\infty}^\infty \hat{a}(k)e^{i[kx-\omega(k)t]}dk, \quad (4.12a,b)$$

where all spectral terms satisfy the linear dispersion relationship $\omega = \sqrt{g|k|}$ and $\hat{a}(k) = i|k|\hat{b}(k)/\omega(k)$ in order to satisfy the (linearized in α) free surface boundary conditions (2.3-2.2a). For consistency with the separation of scales approach, we choose $\hat{b}(k)$ so that $\phi^{(1)}(x, z=0, t)$ in (4.12) has a Gaussian spatial distribution equivalent to (3.2), namely $\hat{b}(k) = (\sigma b_0/\sqrt{2\pi})\exp(-\sigma^2(k-k_0)^2/2)$. In turn, we set $b_0 = -i\omega_0 a_0/k_0$, so that the surface elevation envelope is focussed at $x=0$ and $t=0$. We let f denote the Gaussian wave number spectrum with unit amplitude: $f(k) = (\sigma/\sqrt{2\pi})\exp(-\sigma^2(k-k_0)^2/2)$.

(i) Stokes drift and transport for fully dispersive wave groups $O(\alpha^2\epsilon^\infty)$

By substituting linear expressions for $\partial u^{(1)}/\partial x$, $\partial u^{(1)}/\partial z$, $\Delta x^{(1)}$ and $\Delta z^{(1)}$ obtained from (4.12a) into $d\mathbf{x}/dt = \mathbf{u}(\mathbf{x}, t)$, we obtain for the horizontal Stokes drift up to 2nd order in steepness:

$$u_{\text{SD}}(x, z, t) = \frac{|b_0|^2}{2}\int_{-\infty}^\infty\int_{-\infty}^\infty f(k_1)f(k_2)\frac{k_1^2k_2+k_1|k_1||k_2|}{\omega(k_2)}e^{(|k_1|+|k_2|)z}\cos(\theta_2-\theta_1)dk_1dk_2, \quad (4.13)$$

where $\theta_j = k_j x - \omega_j t + \mu_j$ for $j=1, 2$. Although (4.13) does not appear to have a closed form solution, it can be readily confirmed that it reduces to (4.1) in the limit of narrow band-width ($\epsilon \ll 1$). Finally, we note we have deliberately chosen a continuous over a discrete spectral representation, so that the (small) Lagrangian displacements can be evaluated to the required accuracy using standard numerical integration techniques and the solutions without dispersion (§4(a)) and with leading-order dispersion (§4(b)) can be recovered in the limit of small ϵ . For the same reason and to allow for Gaussian groups, we have allowed for both positive and negative wave numbers, although the contribution from the latter is numerically negligibly small for the bandwidth considered herein ($\epsilon = 0.16$).

(ii) Return flow for fully dispersive wave groups $O(\alpha^2 \epsilon^\infty)$

By substituting the linear solutions (4.12), the right hand side of (3.8) becomes:

$$\left(\frac{\partial}{\partial z} + \frac{1}{g} \frac{\partial^2}{\partial t^2}\right) \phi_{\text{RF}}^{(2)} = \frac{|b_0|^2}{2} \int_{-\infty}^{\infty} \int_{-\infty}^{\infty} \frac{f(k_1)f(k_2)(\sqrt{|k_1|} - \sqrt{|k_2|})(|k_1||k_2| + k_1k_2)}{\sqrt{g}} \sin(\theta_2 - \theta_1) dk_1 dk_2. \quad (4.14)$$

The solution to Laplace subject to the “forcing” (4.14) and the bottom boundary condition is then:

$$\phi_{\text{RF}}(x, z, t) = \frac{|b_0|^2}{2\sqrt{g}} \int_{-\infty}^{\infty} \int_{-\infty}^{\infty} \frac{f(k_1)f(k_2)(\sqrt{|k_1|} - \sqrt{|k_2|})(|k_1||k_2| + k_1k_2)}{|k_2 - k_1| - (\sqrt{|k_2|} - \sqrt{|k_1|})^2} e^{|k_2 - k_1|z} \sin(\theta_2 - \theta_1) dk_1 dk_2. \quad (4.15)$$

For a spectrum with only positive wave numbers, (4.15) reduces to the more familiar (see the deep-water limit of Longuet-Higgins & Stewart (1962) evaluated explicitly by Sharma & Dean (1981) and Dalzell (1999)):

$$\phi_{\text{RF}}(x, z, t) = \int_0^{\infty} \int_{k_2 > k_1}^{\infty} \hat{a}(k_1)\hat{a}(k_2)\omega(k_2)e^{(k_2 - k_1)z} \sin(\theta_2 - \theta_1) dk_2 dk_1. \quad (4.16)$$

In §4(b) we have already shown that leading-order frequency dispersion does not affect the Stokes drift velocities. It is evident from figure 2a that for reasonable values of the bandwidth ($\epsilon = 0.16$) the effect of full dispersion is negligible too. Focussing on the return flow, it has been shown in §4(b) that leading-order dispersion generally increases the magnitude of the horizontal return flow velocities. It can be confirmed from figure 2b that leading-order dispersion is in good agreement with full dispersion for $\epsilon = 0.16$. The effect remains small with magnitudes of the return flow velocity at $z = 0$ approximately 10% larger at the centre of the group (figure 2b) and 7% at $x = \pm\sqrt{2}\sigma$ when allowing for dispersion.

The physical explanation for the larger return flow velocities is most easily understood by considering the “forcing” equation (3.9). Without any dispersion ($O(\epsilon)$) (3.9) is simply a steady mass balance argument: the divergence of the volume flux on the right hand side results in an up- and downflow on either side of the group. Including leading-order dispersion ($O(\epsilon^2)$), the “forcing”-term on the right hand side of (3.9) is not affected. The only difference is that the problem is no longer steady as the group disperses and an extra term is introduced on the left hand side. In loose terms, although the volume deficit and excess associated with the Stokes transports remains unaffected, on the same time scale the group appears to have become more broad spatially thus requiring larger return flow velocities to “return” the fluid and ensure the total induced mean flow, the sum of the Stokes transport and the return flow, is divergence free.

5. Particle trajectories

In this section we use the kinematics for groups without dispersion, with leading-order dispersion and a fully dispersive wave group evaluated in §4(a)-§4(c) to determine the scaling and shape of the Lagrangian particle trajectories at and below the free surface, as well as their final displacements. The total Lagrangian velocity of a particle \mathbf{u}_L is determined by the sum of its Stokes drift \mathbf{u}_{SD} and the Eulerian return flow field \mathbf{u}_{RF} :

$$\underbrace{\mathbf{u}_L}_{\text{Lagrangian}} = \underbrace{\mathbf{u}_{\text{SD}}}_{\text{Stokes drift}} + \underbrace{\mathbf{u}_{\text{RF}}}_{\text{Euler}}. \quad (5.1)$$

We first consider the net contribution by each in turn.

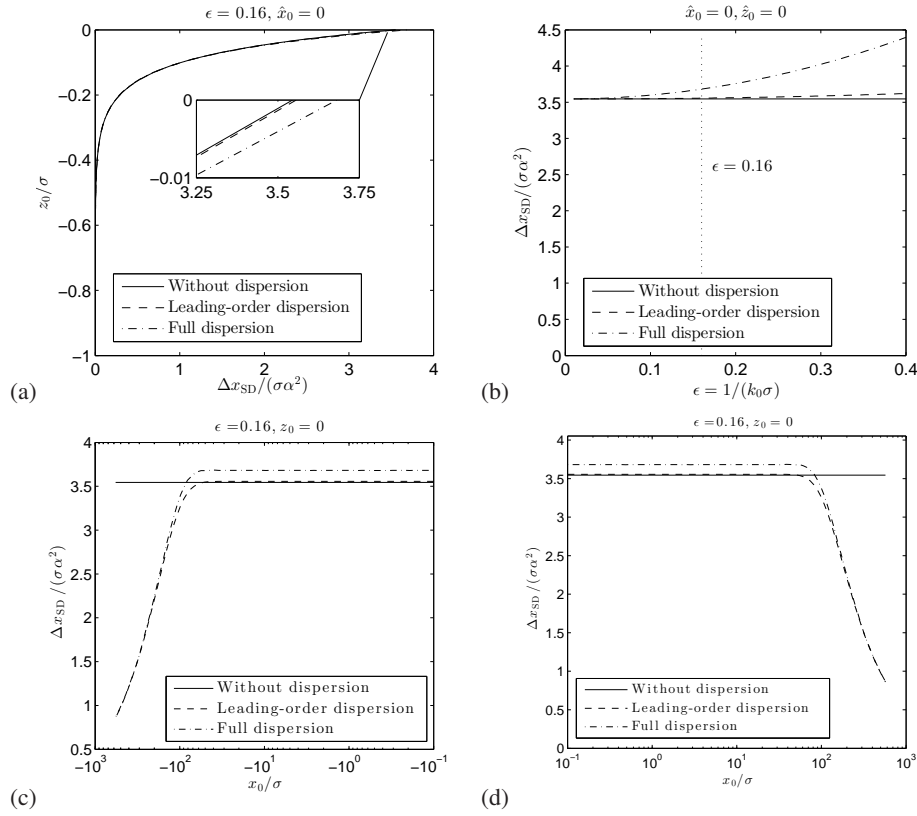


Figure 3. Net horizontal particle displacement due to Stokes drift Δx_{SD} (a) as a function of depth, (b) as a function of the bandwidth parameter ϵ and (c,d) as a function of the initial position of the particle x_0 relative to the focus point of the group $x = 0$ (at $t = 0$) for (c) negative x_0 and (d) positive x_0 . Three solutions are compared in each panel: the separation of scales solution without dispersion (5.2), with leading-order dispersion (5.3) and the Fourier-space solution with full dispersion. The three solutions in (c,d) are in fact symmetric around $x_0 = 0$.

(a) Particle displacement by Stokes drift

From (4.1a) we obtain for the net horizontal displacement due to Stokes drift for a particle as a function of its initial vertical position z_0 and for a Gaussian group:

$$\frac{\Delta x_{SD}(z_0)}{\sigma} = \frac{\int_{-\infty}^{\infty} u_{SD}(x_0, z_0, t) dt}{\sigma} = 2\sqrt{\pi}\alpha^2 e^{2k_0 z_0} \quad \text{without dispersion,} \quad (5.2)$$

where we have ignored the effects of dispersion. The horizontal particle displacement is thus only a function of the steepness (cf. α^2) and the half-width of the wave group σ , but decays rapidly with depth, as would be expected. Including the leading-order effect of dispersion, we obtain from (4.1) in combination with the leading-order dispersive group (4.10):

$$\frac{\Delta x_{SD}(x_0, z_0)}{\sigma} = 2\alpha^2 e^{2k_0 z_0} \int_{-\infty}^{\infty} \frac{1}{\sqrt{1 + \epsilon^2 \hat{t}^2/4}} e^{\frac{-(\hat{x}_0 - \hat{t})^2}{1 + \epsilon^2 \hat{t}^2/4}} d\hat{t} \quad \text{with leading-order dispersion,} \quad (5.3)$$

where the right-hand side integral has been non dimensionalized by defining $\hat{x}_0 = x_0/\sigma$ and $\hat{t} = c_{g,0}t/\sigma$. The net horizontal displacement due to Stokes drift is now both a function of the initial horizontal and the initial vertical position of the particle. Finally, the fully dispersive solution (4.13) can be integrated numerically. Figure 3 compares the three solutions. It is evident then from figure 3a that dispersion does

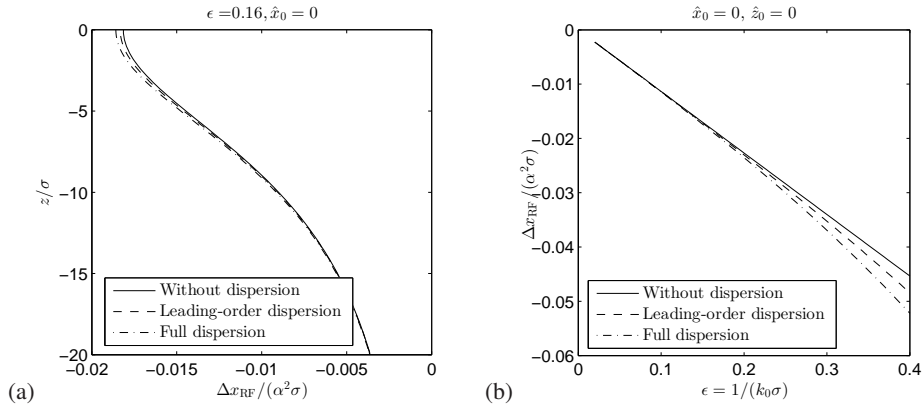


Figure 4. Net horizontal particle displacement due to the return flow Δx_{RF} (a) as a function of depth and (b) as a function of the bandwidth parameter ϵ . Three solutions are compared in each panel: the separation of scales solution without dispersion, with leading-order dispersion and the Fourier-space solution with full dispersion.

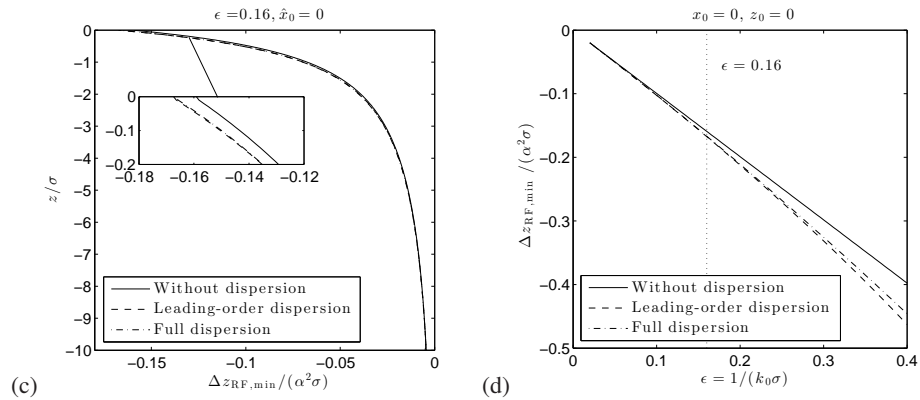


Figure 5. Maximum vertical particle displacement due to the return flow $\Delta z_{\text{RF,min}}$ (a) as a function of depth and (b) as a function of the bandwidth parameter ϵ . Three solutions are compared in each panel: the separation of scales solution without dispersion, with leading-order dispersion and the Fourier-space solution with full dispersion.

not non-negligibly affect the horizontal displacement by Stokes drift for $\epsilon = 0.16$. In fact, the effects of dispersion only become apparent at very high ϵ (figure 3b). These differences then arise from higher-order and not leading-order dispersion (figure 3b). Particles located very far away from the centre of the group ($|x_0|/\sigma \gtrsim 10^2$) simply undergo motion corresponding to a group that has dispersed and is of much reduced amplitude (figures 3c,d).

(b) Particle displacement by the return flow

From the identity of the Stokes transport and the opposite and equal return flow volume flux $Q_{\text{ST}}(x, t) = -Q_{\text{RF}}(x, t)$ for a non-dispersive wave group, it follows that equal and opposite (two-dimensional) volumes

of fluid V_{ST} and V_{RF} are transported horizontally by each:

$$\underbrace{\int_{-\infty}^{\infty} Q_{ST}(x, t) dt}_{\equiv V_{ST}} = - \underbrace{\int_{-\infty}^{\infty} Q_{RF}(x, t) dt}_{\equiv V_{RF}}. \quad (5.4)$$

The horizontal transport by the return flow can be found by integrating the horizontal return flow velocity with respect to time. For a wave group without dispersion we obtain from (4.3):

$$\frac{\Delta x_{RF}(z_0)}{\sigma} = -\frac{\alpha^2 \varepsilon}{\sqrt{\pi}} \int_{-\infty}^{\infty} \int_0^{\infty} \hat{k} e^{-\frac{\hat{k}^2}{4} + \hat{k} \hat{z}_0} \cos(\hat{k} \hat{t}) d\hat{k} d\hat{t} \quad \text{without dispersion}, \quad (5.5)$$

where the double integral on the right hand side is non-dimensional with $\hat{k} = k\sigma$, $\hat{t} = c_{g,0}t/\sigma$ and only a function of the scaled depth $\hat{z}_0 = z_0/\sigma$. Explicitly, we have from numerical evaluation of the double integral for a particle located at $z_0 = 0$:

$$\frac{\Delta x_{RF}(z_0 = 0)}{\sigma} \approx -0.1134\alpha^2 \varepsilon \quad \text{without dispersion}. \quad (5.6)$$

From comparison of (5.2) and (5.6) for $z_0 = 0$ we thus have a positive horizontal displacement due to Stokes drift that is a factor $\approx 31.3/\varepsilon$ (≈ 195 for $\varepsilon = 0.16$) larger compared to the opposite horizontal displacement due to the return flow. Equation (5.5) can be readily modified to allow for the effects of leading-order dispersion. From (4.11) we obtain:

$$\frac{\Delta x_{RF}(x_0, z_0)}{\sigma} = -\frac{\alpha^2 \varepsilon}{\sqrt{\pi}} \int_{-\infty}^{\infty} \int_0^{\infty} \frac{\hat{k}}{1 - \varepsilon \hat{k}/4} e^{-\frac{\hat{k}^2}{4} + \hat{k} \hat{z}_0} \cos(\hat{k}(\hat{x}_0 - \hat{t})) d\hat{k} d\hat{t} \quad \text{with leading-order dispersion}, \quad (5.7)$$

which is now additionally a function of the non-dimensional initial horizontal position $\hat{x}_0 = x_0/\sigma$. Finally, the net horizontal displacement by the fully dispersive return flow can be obtained by means of numerical integration of the horizontal velocity corresponding to (4.15).

It turns out that the double integrals in (5.5) and (5.7) are very difficult to evaluate using standard numerical quadratures in part due to the very slow decay of the large time tails of the integrand (cf. $u_{RF} \sim t^{-2}$, see appendix B). The horizontal displacements are in practice evaluated by first calculating the depth-integrated transported volume $V_{RF}(z_0) = \int_{-\infty}^{z_0} u_{RF} dz$ as a function of initial particle depth z_0 followed by numerical differentiation of this quantity with respect to z_0 . An alternative method that gives the same result is to integrate numerically for small time and analytically for large time using the far-field solutions in appendix B and combine both contributions.

Figure 4a then shows the net horizontal displacement as a function of depth displaying an even slower variation than the horizontal return flow velocity (figure 2a,c). The (small) magnitude of the displacement at $z = -10\sigma$ is still approximately half the value at the still water level. It can be shown that the far-field solution (4.7) does not result in a net displacement (appendix B). In agreement with the larger return flow velocities in figure 2b dispersion slightly increases the magnitude of the (negative) displacement (figure 4a) and more so for large ε (figure 4b). We emphasize that, as opposed to the Stokes drift, the net displacement due to the return flow for non-dispersive groups is not a direct function of σ , but the dependence is only through the dependence on the vertical position z_0/σ , which scales on σ . The small parameter ε only appears in (5.5) because of the scaling of the left hand side by σ . It goes without saying that the depth integral of the displacement due to Stokes drift and the return flow despite their very different distribution with depth are equal and opposite (5.4). A very small backwards displacement that decays extremely slowly with depth thus compensates a very much larger forward displacement concentrated near the still water level.

Although no net vertical displacement of particles arises due to the return flow, we can evaluate the maximum vertical displacement to obtain a sense of the vertical scale of the motion associated with the

return flow. At $z_0 = 0$ we have from (4.4):

$$\frac{\Delta z_{\text{RF,min}}(z_0 = 0)}{\sigma} = -\alpha^2 \epsilon \quad \text{without dispersion,} \quad (5.8)$$

and similarly for the leading-order and fully dispersive solution. Figure 5 evaluates this maximum vertical displacement as a function of depth and ϵ . We note from comparison of figures 4a and 5a that the maximum vertical displacement is approximately 10 times larger than the net horizontal displacement.

(c) Lagrangian trajectories

Having obtained expressions for the net displacement due to Stokes drift and the return flow, figure 6 shows the trajectories of Lagrangian particles obtained from numerical integration of the equations of motion $d\mathbf{x}/dt = \mathbf{u}^{(1)} + \mathbf{u}^{(2)}$ for a group without dispersion for particles initially located at different depths (rows) and different values of ϵ (columns). The behaviour of particles with initial positions at the still water level (top row) is dominated by Stokes drift with smaller values of ϵ corresponding to more individual waves making up the group and thus more orbits contributing to the net horizontal displacement. For particles at great depth (bottom row) the particle trajectories are dominated by the return flow with the individual waves only giving rise to small deflections of the horse-shoe shaped particle trajectory. We note that for deep water the magnitude of the horse-shoe shaped return flow trajectory is in fact very small, so small in fact that it might be difficult to observe in reality. At intermediate depths both the effect of Stokes drift and the return flow play a role.

6. Conclusions

The Lagrangian trajectories of neutrally buoyant particles underneath focussed surface gravity wave groups have been examined and simple leading-order expressions for the net displacement resulting from Stokes drift and the return flow have been developed. In the deep-water limit, both the Stokes drift, the mean velocity that arises due to the waves when tracking Lagrangian particles, and the Stokes transport, the Eulerian volume flux that arises at the same order (second order) in steepness, occur in the vicinity of the still water level. The much smaller return flow, on the other hand, varies much more slowly with depth, to the extent that its variation in the near surface region, where Stokes drift takes place, can be ignored. A separation of the physical domains in which the two physical phenomena occur thus takes place. Frequency dispersion is found to only marginally affect both phenomena for realistic sea states. To good approximation, the problem can be studied using a leading-order WKB approximation, in which the wave-induced mean flow is steady in the frame of reference of the group without resorting to more complicated frequency domain representations (Dalzell, 1999; Longuet-Higgins & Stewart, 1962; Sharma & Dean, 1981). To obtain a sense of the magnitude of the displacements in real seas, figure 7, shows the particle displacements predicted as a function of the peak period of the spectrum T_0 for a group with linear wave height $H_0 = 2a_0 = 10\text{m}$. Whereas displacements of the order $10^1\text{--}10^2\text{m}$ are predicted for the Stokes drift, the return flow only results in displacements of the order $10^{-2}\text{--}10^{-1}\text{m}$.

The results presented herein rely crucially on the deep-water assumption. Although a typical engineering criterion for an oscillatory wave to be in deep water is $k_0 d \gtrsim 3$, a much larger depth may be required for the return flow of a group not to “feel” the presence of the bottom. For example, for $\epsilon = 0.16$, we have $k_0 d = 3$ corresponding to $d/\sigma = 3\epsilon = 0.48$, whereas the Lagrangian displacement due to the return current may still be a significant share of its surface value at $z/\sigma = -20$ (cf. figure 4a). A sea that is deep for a $T_0 = 10\text{ s}$ wave, namely $d \approx 75\text{ m}$ so that $k_0 d = 3$, may require a much greater depth for the return flow to be unaffected by the bottom boundary condition, namely $d \gtrsim 3\text{ km}$ (taking $z/\sigma = -20$ as a criterion with $\epsilon = 0.16$). The presence of the bottom boundary in what can reasonably be considered infinite depth for the oscillatory components of the wave group but is in fact finite depth for the return flow, is then likely to increase the magnitude of the return flow near the still water level. Taking into account the bottom boundary condition for a seemingly deep sea ($d > 1000\text{ m}$), could help explain part of the discrepancy between measurements and irrotational theory reported in Smith (2006), who present field measurements of the mass transport by

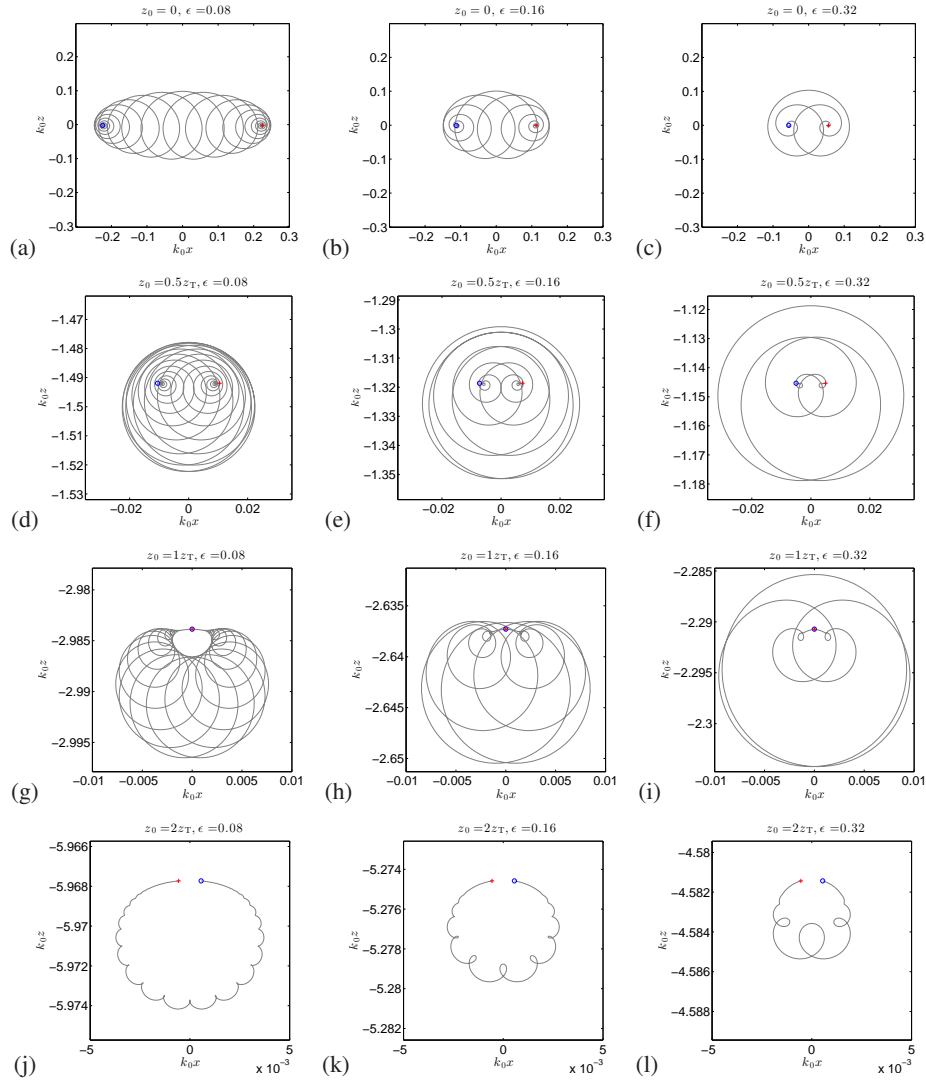


Figure 6. Lagrangian trajectories of neutrally buoyant particles at different depths below a focussed crest wave group and for different values of the bandwidth parameter $\epsilon = 1/(k_0\sigma)$. The rows correspond to initial particle depths $z_0 = \{0, 0.5, 1, 2\}z_T$ with z_T denoting the approximate transition depth (D.3), where the net horizontal Lagrangian transport is zero (see appendix D). The columns correspond to values of $\epsilon = 0.08, 0.16$ and 0.32 , respectively. The trajectories shown correspond to the solutions without dispersion with the blue open circle corresponding to the initial position of the particle and the red cross corresponding to the final position of the particle. The waves are of steepness $\alpha = 0.1$.

wave groups.

Motivated by differences between observations and predictions, Gnanadesikan & Weller (1995) discuss the validity of their assumption of an infinite surface wave field. In practice, the wave field often has a group-like structure and both the Stokes drift and the additionally present return flow will exert a body force on the fluid in the presence of a Coriolis force (Gnanadesikan & Weller, 1995). Consequently, great care is needed in making assumptions of spatial uniformity of the wave-averaged flow fields to derive the

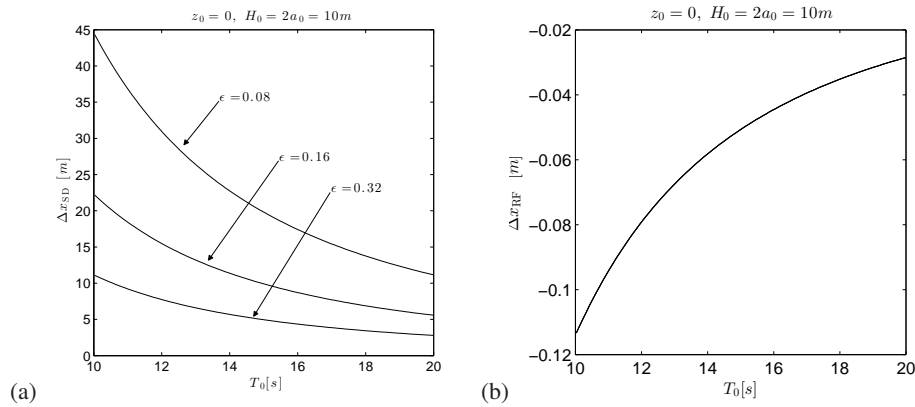


Figure 7. Dimensional net horizontal particle displacement at the surface $z_0 = 0$ (a) due to Stokes drift and (b) due to the return flow as a function of the peak period of the spectrum T_0 for a wave group with linear wave height $H_0 = 2a_0 = 10\text{m}$. Note that solutions are only plotted for $\alpha < 0.2$ corresponding to $T_0 > 2\pi\sqrt{a_0/(g\alpha)} \approx 10.0\text{s}$. The solution in (a) is a function of ϵ , the solution in (b) is not.

equations of motion suitable to describe Langmuir circulation (Thorpe, 2004). Such equations evidently also include Coriolis and buoyancy forcing (see McWilliams & Fox-Kemper (2013)). The results presented herein show that the magnitude of the return flow near the surface from spatial divergence of the Stokes transport alone is likely to be small, but only provided the water is truly deep: $d/\sigma \gg 1$, where σ is the characteristic scale of the group. The depth-integrated induced volume fluxes, however, remain equal and opposite, as cannot be emphasized enough (McIntyre, 1981). In any case, the effects of frequency dispersion of the wave groups on the mass transport can be probably be ignored.

The enhanced return flow has important effects on the stability properties of the wave train through interaction with the mean flow as first captured by Dysthe (1979) for truly infinite depth (see Janssen (1983) for a discussion) and first extended to finite depth by Brinch-Nielsen & Jonsson (1986) and more recently in an Hamiltonian framework by Craig *et al.* (2010) and Gramstad & Trulsen (2007). On finite depth the return flow enters the non-linear Schrödinger equation describing the evolution and stability of the group at lower order than on deep water. As a final caveat, we note that, although the results presented herein for Gaussian spectra can be readily extended to different spectra, they rely on ignoring the third dimension evidently present in real seas, which will further reduce the magnitude of the the return flow. Our finding herein that the effect of frequency dispersion is only small in deep water provides a justification for the assumption made in van den Bremer & Taylor (2015) that this is the case for general water depth and directionally spread seas. Furthermore, estimating real, that is directional and broad-banded, spectra from observations remains an area of considerable interest (Breivik *et al.*, 2016; Webb & Fox-Kemper, 2015). Thus, including the return flow in such estimates, resulting in more realistic estimates of net transport, provides ample scope for future work. In the truly deep-water limit for wave groups ($k_0 d \gg 1$ and $d/\sigma \gg 1$), the return flow is shown to play only a very small role and other otherwise small physical effects such as weak stratification, viscosity and Coriolis forcing may become just as important.

A. Derivation of (4.5)

From (4.3), we obtain the non-dimensional integral:

$$\hat{u}_{\text{RF}}(x = c_{g,0}t) = -\frac{1}{2} \int_0^\infty e^{-\frac{\hat{k}^2}{4} + \hat{k}\hat{z}} \hat{k} d\hat{k} = -\frac{1}{2} e^{\hat{z}^2} \int_{-2\hat{z}}^\infty e^{-\frac{(\hat{k}^*)^2}{4}} (\hat{k}^* + 2\hat{z}) d\hat{k}^* = -(1 + \sqrt{\pi}\hat{z}(1 + \text{erf}(\hat{z}))e^{\hat{z}^2}), \quad (\text{A } 1)$$

where $\hat{u}_{\text{RF}} \equiv u_{\text{RF}}/(\omega_0|a_0|^2/\sqrt{\pi}\sigma)$, $\hat{k} = k\sigma$ and $\hat{z} = z/\sigma$. The first identity follows from the quadratic relationship $-\hat{k}^2/4 + \hat{k}\hat{z} = -(\hat{k} - 2\hat{z})^2/4 + \hat{z}^2$ and a change of variables $\hat{k}^* = \hat{k} - 2\hat{z}$ and the second identity from evaluation of two standard integrals.

B. Far-field asymptotics in wave number space

(a) Without dispersion

From (4.3) the horizontal component of the return flow without dispersion can be expressed in terms of the non-dimensional integral:

$$\frac{u_{\text{RF}}(x, z, t)}{-\frac{1}{2\sqrt{\pi}}\frac{|a_0|^2\omega_0}{\sigma}} = \text{Re} \left[\int_0^\infty f(\hat{k}) e^{\hat{k}(\hat{z} + i(\hat{x} - \hat{t}))} d\hat{k} \right], \quad (\text{A } 1)$$

where $\hat{k} = k\sigma$, $\hat{z} = z/\sigma$, $\hat{x} = x/\sigma$ and $\hat{t} = c_{g,0}t/\sigma$ and $f(\hat{k}) = \hat{k} \exp(-\hat{k}^2/4)$. The asymptotic behaviour of the horizontal component of the return flow without dispersion (A 1) at large distances away from the centre of the group, either $|x - c_{g,0}t| \rightarrow \infty$, $z \rightarrow -\infty$ or both, can be found by integrating by parts twice:

$$\text{Re} \left[\int_0^\infty f(\hat{k}) e^{\hat{k}(\hat{z} + i(\hat{x} - \hat{t}))} d\hat{k} \right] = -\frac{(\hat{x} - \hat{t})^2 - \hat{z}^2}{((\hat{x} - \hat{t})^2 + \hat{z}^2)^2} + \text{Re} \left[\int_0^\infty \frac{f''(\hat{k}) e^{\hat{k}(\hat{z} + i(\hat{x} - \hat{t}))}}{(\hat{z} + i(\hat{x} - \hat{t}))^2} d\hat{k} \right], \quad (\text{A } 2)$$

where we have used $f(\hat{k}) \rightarrow 0$ as $\hat{k} \rightarrow 0$, $f(\hat{k}) \rightarrow 0$ as $\hat{k} \rightarrow \infty$, $f'(\hat{k}) \rightarrow 1$ as $\hat{k} \rightarrow 0$ and $f'(\hat{k}) \rightarrow 0$ as $\hat{k} \rightarrow \infty$. The Riemann-Lebesgue lemma now guarantees that the right-hand integrals in the final equation of (A 2) converges to zero as $|\hat{x} - \hat{t}| \rightarrow \infty$. For $\hat{z} \rightarrow -\infty$ convergence to zero is guaranteed by the nature of the exponential, so that we have in the far-field ($|\hat{x} - \hat{t}| \rightarrow \infty$ or $\hat{z} \rightarrow -\infty$):

$$u_{\text{RF}}(x, z, t) = \frac{1}{2\sqrt{\pi}} \frac{|a_0|^2\omega_0}{\sigma} \frac{(\hat{x} - \hat{t})^2 - \hat{z}^2}{((\hat{x} - \hat{t})^2 + \hat{z}^2)^2}. \quad (\text{A } 3)$$

From (A 3) we can obtain an expression for the horizontal particle displacement by the return flow in the far-field as a function of time and the initial particle position (x_0, z_0):

$$\frac{\int_{-\infty}^t u_{\text{RF}}(x_0, z_0, t) dt}{\sigma} = \frac{1}{2\sqrt{\pi}} \frac{|a_0|^2\omega_0}{c_{g,0}\sigma} \frac{\hat{x}_0 - \hat{t}}{((\hat{x}_0 - \hat{t})^2 + \hat{z}_0^2)^2}. \quad (\text{A } 4)$$

It is also evident from (A 4) that the net particle transport (by taking the limit $\hat{t} \rightarrow \infty$) by the far field of the return flow is zero.

(b) Without leading-order dispersion

Including the leading-order effect of dispersion (cf. (A 1)), the expression for the horizontal velocity has the same functional form as for a group without dispersion, but with a different function f , which is now given by $f(\hat{k}) = \hat{k} \exp(-\hat{k}^2/4)/(1 - \hat{k}\epsilon/4)$. It can be shown that the new f has the same properties: $f(\hat{k}) \rightarrow 0$ as $\hat{k} \rightarrow 0$, $f(\hat{k}) \rightarrow 0$ as $\hat{k} \rightarrow \infty$, $f'(\hat{k}) \rightarrow 1$ as $\hat{k} \rightarrow 0$ and $f'(\hat{k}) \rightarrow 0$ as $\hat{k} \rightarrow \infty$. The asymptotic argument in §B(a) remains valid and we have for the far field:

$$u_{\text{RF}}(x, z, t) = \frac{|\tilde{a}_0|^2\tilde{\sigma}\omega_0}{2\sqrt{\pi}} \frac{(x - c_{g,0}t)^2 - z^2}{((x - c_{g,0}t)^2 + z^2)^2}, \quad (\text{A } 5)$$

with $|\tilde{a}_0| = |a_0|(1 + \gamma_0^2 t^2/\sigma^4)^{-1/4}$ replacing $|a_0|$ and $\tilde{\sigma} = (1 + \gamma_0^2 t^2/\sigma^4)^{1/2}$ replacing σ in (A 3). We note that $|\tilde{a}_0|^2\tilde{\sigma} = |a_0|^2\sigma$ and that leading-order dispersion thus does not affect the far-field solution.

C. Far-field asymptotics in physical space

Although the solution can be shown to be identical, it may be more physically intuitive to consider the flow field of a series of sources and sinks, in which case we can construct an expression in terms of a summation (over the different sources and sinks) in physical and not wave number space. Instead of integrating (4.4),

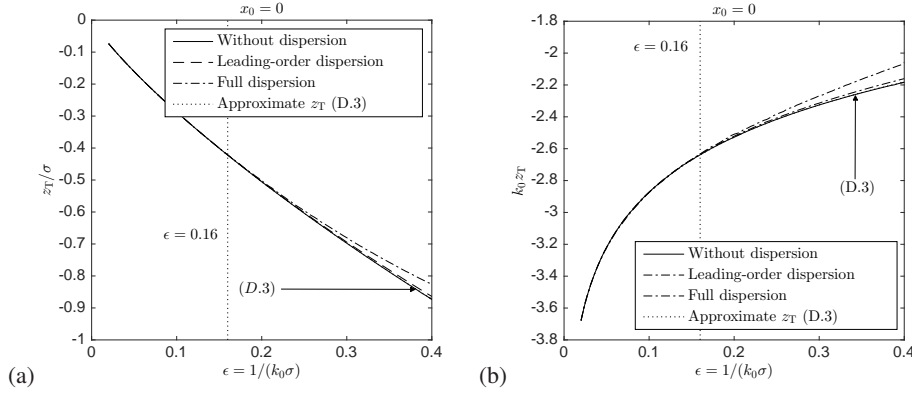


Figure 8. The transition depth between positive horizontal particle transport by the Stokes drift and negative horizontal particle transport by the return flow. Note all the lines (almost) overlap.

we first assume the source and sink are far away from our point of interest (x, z) relative to the distance between the source and sink pair, namely $|x - c_{g,0t}| \gg 2l$, $z \gg 2l$ or both. In this limit (4.4) becomes:

$$du_{\text{RF}} = \frac{2l}{\pi} \frac{(x - c_{g,0t})^2 - z^2}{((x - c_{g,0t})^2 + z^2)^2} M(l) dl, \quad (\text{C.1})$$

where the strength is given by $M = (\omega_0 |a_0|^2 / \sigma) (l / \sigma) \exp(-(l / \sigma)^2)$. Normalizing by the group half-width σ so that $\hat{l} = l / \sigma$, $\hat{x} = x / \sigma$, $\hat{z} = z / \sigma$, we have for the far-field behaviour of a Gaussian group:

$$u_{\text{RF}}(x, z, t) = \frac{2}{\pi} \frac{|a_0|^2 \omega_0}{\sigma} \frac{(\hat{x} - \hat{l})^2 - \hat{z}^2}{((\hat{x} - \hat{l})^2 + \hat{z}^2)^2} \underbrace{\int_0^\infty \hat{l}^2 e^{-\hat{l}^2} d\hat{l}}_{=\sqrt{\pi}/4} = \frac{1}{2\sqrt{\pi}} \frac{|a_0|^2 \omega_0}{\sigma} \frac{(\hat{x} - \hat{l})^2 - \hat{z}^2}{((\hat{x} - \hat{l})^2 + \hat{z}^2)^2}, \quad (\text{C.2})$$

which is equivalent to (A 3).

D. The transition depth

In order to classify when either type of motion described in §5(c) occurs, a transition depth z_T can be defined as the depth at which the positive horizontal displacement of a particle by the Stokes drift is equal to the negative horizontal displacement of a particle by the return flow so that the net Lagrangian displacement is zero:

$$\Delta x_L(z_0 = z_T) = \Delta x_{\text{SD}}(z_0 = z_T) + \Delta x_{\text{RF}}(z_0 = z_T) = 0 \quad \text{transition depth.} \quad (\text{D.1})$$

Above this depth ($z_0 > z_T$) particles will be transported in the direction of positive x and below this depth ($z_0 < z_T$) particles will be transported in the opposite direction. Ignoring the generally small effects of dispersion and making use of the fact that Stokes drift decays much faster with depth than the return flow, an approximate expression for the transition depth $z_{T, \text{APPROX}}$ can be obtained by finding the depth at which the net horizontal Stokes drift displacement (5.2) has decreased to the surface value of the return flow displacement at $z_0 = 0$ (5.6), which is assumed not to decay over that same depth:

$$\Delta x_{\text{RF}}(z_0 = 0) + \Delta x_{\text{SD}}(z_0 = z_{T, \text{APPROX}}) = 0, \quad (\text{D.2})$$

which has the solution:

$$\frac{z_{T, \text{APPROX}}}{\sigma} \approx \frac{1}{2} \epsilon (-3.442 + \log(\epsilon)), \quad \text{or} \quad k_0 z_{T, \text{APPROX}} \approx \frac{1}{2} (-3.442 + \log(\epsilon)). \quad (\text{D.3})$$

Figure 8 compares the approximate transition depth with transition depths obtained from solving $\Delta x_L = 0$ (D.1) implicitly without dispersion, with leading-order dispersion (at $x_0 = 0$) and with full dispersion (at

$x_0 = 0$). It is evident then that the approximate transition depth (D.3) provides an excellent prediction of the actual transition depth even including the effects of dispersion at large values of ϵ , much larger than the representative value of $\epsilon = 0.16$.

As the steepness of the wave $\alpha = |A_0|k_0$ affects both the magnitude of the displacement due to Stokes drift and the displacement due to the return flow in the same way, the transition depth is only a function of the bandwidth parameter $\epsilon = 1/(k_0\sigma)$. As we keep the wave length of the peak spectral component k_0 fixed and shrink the width of the group σ (and thus let ϵ increase), the magnitude of the displacement due to the return flow near the free surface is unaffected $\Delta x_{\text{RF}} \approx -0.1134\alpha^2 k_0^{-1}$ (from (5.6)), but the magnitude of the displacement due to Stokes drift $\Delta x_{\text{SD}} = 2\sqrt{\pi}\sigma\alpha^2 \exp(2k_0 z_0)$ (from (5.2)) decreases, as the group is simply shorter. The point at which the net displacement is equal to zero must then occur at smaller depth and z_T approaches zero as ϵ increases (figure 8b).

Acknowledgements

Authors' contributions T.S.v.d.B. developed the theoretical analysis in the paper as part of his DPhil (2015) supervised by P.H.T.

Competing interests We declare we have no competing interests.

Funding We received no external funding for this study.

References

- Ardhuin, F., Marié, L., Rasche, N., Forget, P. & Roland, A. 2009 Observation and estimation of Lagrangian, Stokes, and Eulerian currents induced by wind and waves at the sea surface. *J. Phys. Oceanogr.*, **39**(11), 2820–2838.
- Belcher, S. E., Grant, A. L. M., Hanley, K. E., Fox-Kemper, B., Roedel, L. V., Sullivan, P. P., Large, W. G., Andy, A. B., Hines, A. *et al.* 2012 A global perspective on Langmuir turbulence in the ocean surface boundary layer. *Geophys. Res. Lett.*, **39**(18).
- Breivik, O., Bidlot, J. & Janssen, P. A. E. M. 2014 Approximate Stokes drift profiles in deep water. *J. Phys. Oceanogr.*, **44**, 2433–2445.
- Breivik, O., Bidlot, J. & Janssen, P. A. E. M. 2016 A Stokes drift approximation based on the Phillips spectrum. *Ocean Model.*, **100**, 49–56.
- Brinch-Nielsen, P. U. & Jonsson, I. G. 1986 Fourth order evolution-equations and stability analysis for Stokes waves on arbitrary water depth. *Wave Motion*, **8**(455).
- Craig, W., Guyenne, P. & Sulem, C. 2010 A Hamiltonian approach to nonlinear modulation of surface water waves. *Wave Motion*, **47**(552).
- Craik, A. D. D. & Leibovich, S. 1976 A rational model for Langmuir circulations. *J. Fluid Mech.*, **73**, 401–426.
- Dalzell, J. R. 1999 A note on finite depth second-order wave-wave interactions. *Appl. Ocean Res.*, **21**, 105–111.
- Dysthe, K. 1979 Note on a modification to the nonlinear Schrödinger equation for application to deep water waves. *Proc. R. Soc. Lond. A*, **369**, 105–114.
- Gibbs, R. H. & Taylor, P. H. 2005 Formation of walls of water in fully nonlinear simulations. *Appl. Ocean Res.*, **27**(4), 142–157.
- Gnanadesikan, A. & Weller, R. A. 1995 Structure and instability of the Ekman spiral in the presence of surface gravity waves. *J. Phys. Oceanogr.*, **25**, 3148–3171.
- Gramstad, O. & Trulsen, K. 2007 Hamiltonian form of the modified nonlinear Schrödinger equation for gravity waves on arbitrary depth. *J. Fluid Mech.*, **670**, 404–426.
- Groeneweg, J. & Klopman, G. 1998 Changes of the mean velocity profiles in the combined wave-current motion described in a GLM formulation. *J. Fluid Mech.*, **370**, 271–269.
- Hasselmann, D. E., Dunckel, M. & Ewing, J. A. 1980 Directional wave spectra observed during JONSWAP 1973. *J. Phys. Oceanogr.*, **10**, 1264–1280.

- Hudspeth, R. T. & Sulisz, W. 1991 Stokes drift in two-dimensional wave flumes. *J. Fluid Mech.*, **230**, 209–229.
- Janssen, P. A. E. M. 1983 On a fourth-order envelope equation for deep-water waves. *J. Fluid Mech.*, **126**, 1–11.
- Kantha, L. H. & Clayson, C. A. 2004 On the effect of surface gravity waves on mixing in the oceanic mixed layer. *Ocean Model.*, **6**, 101–124.
- Kinsman, B. 1984 *Wind waves: their generation and propagation on the ocean surface*. New York, USA: Dover.
- Longuet-Higgins, M. 1953 Mass transport in water waves. *Phil. Trans. R. Soc. Lond. A*, **245**, 535–581.
- Longuet-Higgins, M. & Stewart, R. 1962 Radiation stress and mass transport in gravity waves, with applications to ‘surf beats’. *J. Fluid Mech.*, **13**, 481–504.
- Longuet-Higgins, M. & Stewart, R. 1964 Radiation stresses in water waves; a physical discussion, with applications. *Deep-sea Res.*, **2**, 529–562.
- McIntyre, M. E. 1981 On the wave momentum myth. *J. Fluid Mech.*, **106**, 331–347.
- McWilliams, J. C. & Fox-Kemper, B. 2013 Oceanic wave-balanced surface fronts and filaments. *J. Fluid Mech.*, **730**, 464–490.
- McWilliams, J. C. & Restrepo, J. 1999 The wave-driven ocean circulation. *J. Phys. Oceanogr.*, **29**, 2523–2540.
- Monismith, S. G., Cowen, E., Nepf, H. M., Magnaudet, J. & Thais, L. 2007 Laboratory observations of mean flows under surface gravity waves. *J. Fluid Mech.*, **573**, 131–147.
- Sharma, J. & Dean, R. G. 1981 Second-order directional seas and associated wave forces. *Proc. Offshore Tech. Conf.*, **4**, 2505–2514.
- Smith, J. A. 2006 Observed variability of ocean wave Stokes drift, and the Eulerian response to passing groups. *J. Phys. Oceanogr.*, **36**, 1381–1402.
- Starr, V. P. 1947 A momentum integral for surface waves in deep water. *J. Mar. Res.*, **6**, 126–135.
- Stokes, G. G. 1847 On the theory of oscillatory waves. *Trans. Camb. Philos. Soc.*, **8**, 441–455.
- Swan, C. 1990 Convection within an experimental wave flume. *J. Hydraul. Res.*, **28**, 273–282.
- Tamura, H., Miyazawa, Y. & Oey, L. Y. 2012 The Stokes drift and wave induced-mass flux in the north Pacific. *J. Geophys. Res.*, **117**.
- Thorpe, S. A. 2004 Langmuir circulation. *Annu. Rev. Fluid Mech.*, **36**, 55–79.
- van den Bremer, T. S. & Taylor, P. H. 2015 Estimates of Lagrangian transport by wave groups: the effects of finite depth and directionality. *J. Geophys. Res.*, **120**(4), 2701–2722.
- van Dyke, M. 1982 *An album of fluid motion*. Stanford, USA: The Parabolic Press.
- Webb, A. & Fox-Kemper, B. 2015 Impacts of wave spreading and multidirectional waves on estimating Stokes drift. *Ocean Model.*, **96**, 49–64.
- Weber, J. E. H. 2011 Do we observe Gerstner waves in wave tank experiments? *Wave Motion*, **48**(4), 301–309.
- Yuen, H. C. & Lake, B. M. 1975 Nonlinear deep water waves: theory and experiment. *Phys. Fluids*, **18**, 956–960.